

## Supporting Information

### Novel flower-like titanium phosphate microstructures and their application in lead ion removal in drinking water

Xueyun Wang,<sup>ab</sup> Xiulin Yang,<sup>ab</sup> Jianhua Cai,<sup>ab</sup> Tingting Miao,<sup>ab</sup> Lihua Li,<sup>ab</sup> Gen Li,<sup>ab</sup>  
Dingrong Deng,<sup>ab</sup> Li Jiang,<sup>\*a</sup> and Chunru Wang<sup>a</sup>

*Beijing National Laboratory for Molecular Sciences, Laboratory of Molecular Nanostructure and Nanotechnology, Institute of Chemistry, Beijing 100190, China. Fax: 86-10-62652120; Tel: 86-10-62652120; E-mail: jiangli@iccas.ac.cn*

### Contents

Experimental Section: The synthesis of titanium phosphate and its adsorption of heavy metal ions.

Characterization: SEM, TEM, XRD, Nitrogen adsorption/desorption isotherm and TGA was used to characterize the sample.

**Fig. S1.** SEM characterization of inner of the sample.

**Fig. S2.** SEM image of the product prepared at (a) 30 °C for 24 h; (b) 30 °C for 48 h; (c) 50 °C for 1 h; (d) 50 °C for 12 h; (e) 80 °C for 4 min; (f) 80 °C for 20 min

**Fig. S3.** XRD patterns of the products prepared at 50 °C of different reaction time (a) 12 h; (b) 24 h; (c) 36 h; (d) 48 h; (e) 60 h; (f) 84 h.

**Fig. S4.** XRD patterns of the products  $\text{Ti}(\text{HPO}_4)_2 \cdot \text{H}_2\text{O}$  before and after calcining at 250 and 700 °C.

**Fig. S5.** (a) pH titration curves of titanium phosphate solution with and without  $\text{Na}^+$  exchanging. (b) plot of the zeta potential of the adsorbents as a function of pH. (c)  $\text{Pb}^{2+}$  removed efficiency of titanium phosphate as a function of pH.

**Fig. S6.** XRD patterns of titanium phosphate before, after adsorption of  $\text{Pb}^{2+}$  and regenerated by HCl.

**Fig. S7.** Titanium and phosphates released in treated water with different  $\text{Pb}^{2+}$  concentrations.

**Table S1.**  $\text{Pb}^{2+}$  remove performance at low lead concentrations.

## **Experimental Section**

**Synthesis of titanium phosphate.** 500  $\mu\text{L}$  tetrabutyl titanate was dissolved in 100 mL dehydrated alcohol and this mixture was stirred for 1 hour at room temperature. Then, 5mL of 85% (w/w) phosphoric acid was added to the above mixture and the solution was stirred at 50  $^{\circ}\text{C}$  for 12 h. The suspension was next centrifuged and the precipitate was washed with distilled water for several times and then dried under vacuum at 50  $^{\circ}\text{C}$ .

**Characterization:** Crystal structures of the sample were examined by a Shimadzu XRD-7000 diffractometer with Cu K radiation ( $\lambda=1.54056 \text{ \AA}$ ). Microscopic features of the sample were characterized by a field emission scanning electron microscope (FE-SEM, JEOL JEM 6701F) and transmission electron microscopy (TEM JEOL 1011). Nitrogen adsorption/desorption isotherm was measured by a Quantachrome Autosorb AS-1 instrument at 77 K and mesopore size was calculated using the Barrett-Joyner-Halenda (BJH) model and density functional theory (DFT) method. Fourier-transform infrared (FTIR) spectra in the frequency between 500 and 4000  $\text{cm}^{-1}$  was collected on a Nicolet iZ10 infrared spectrometer. Thermogravimetric analysis was obtained on a Pyris 1 TGA unit (Perkin-Elmer, USA) under nitrogen

atmosphere at a heating rate of  $10\text{ }^{\circ}\text{C min}^{-1}$ . pH value was measured using pH meter (Thermo Scientific, Model: 410p-13).

**pH titration** :350 mg of flower-like titanium phosphates were mixed with 100 ml of 0.1 M NaCl. This mixture was kept for 4 h and titrated against 0.15 M NaOH solution.<sup>2,3</sup> The pH of the solution was recorded after each addition of 1.0 ml of the titration till the pH became constant. The milliequivalents of  $\text{OH}^{-}$  ion consumed were calculated according to the solution pH values before and after the exchange process. Milliequivalents of  $\text{OH}^{-}$  ions consumed by the exchanger were then plotted against the corresponding pH values to get the pH-titration curves.

**Heavy metal ion adsorption.**  $\text{Pb}(\text{NO}_3)_2$  was used as the sources of heavy metal ions to prepare solutions with  $\text{Pb}^{2+}$  ions concentrations of 10, 20, 50, 100, 250 and  $500\text{ mg}\cdot\text{L}^{-1}$ , and  $\text{Ca}(\text{NO}_3)_2$  as the source of competing cation  $\text{Ca}^{2+}$  ions. The pH value of the  $\text{Pb}(\text{NO}_3)_2$  solutions was adjusted to 5.5 with NaOH or HCl (0.2 M) prior to the adsorption experiments. The adsorption kinetic behaviors were preformed with the initial ion concentration of  $50\text{ mg}\cdot\text{L}^{-1}$  and adsorbent dose for  $20\text{ mg}/100\text{ mL}$ . After a specified time, 5 mL supernatant solutions were pipetted and filtered through  $0.22\text{ }\mu\text{m}$  PTFE membranes. The adsorption isotherms were obtained by adding 5 mg flower-like titanium phosphate into 25 mL  $\text{Pb}(\text{NO}_3)_2$  solutions with different heavy metal ions concentrations and stirred at room temperature. After 12 h the adsorbents were separated through  $0.22\text{ }\mu\text{m}$  PTFE membrane and analyzed by inductively coupled plasma-optical emission spectroscopy (Shimazu ICPE-9000) to measure the remaining metal concentration of ions in the solution. The desorption and

regeneration tests were carried out using 25 mL of a 0.5M HCl solution. The used adsorbents in adsorption kinetics experiments were mixed with the HCl solution and stirring for 12 h. The amount of heavy metals in the supernatant was tested to calculate the desorption efficiency of the adsorbents. The adsorption capacity of the adsorbents was calculated according to the following equation (1):<sup>1</sup>

$$q_e = \frac{(C_0 - C_e)V}{m} \quad (1)$$

Where  $C_0$  and  $C_e$  represent the initial and equilibrium concentrations ( $\text{mg}\cdot\text{L}^{-1}$ ), respectively.  $V$  is the volume (mL) of the solution, and  $m$  is the amount (mg) of adsorbent.

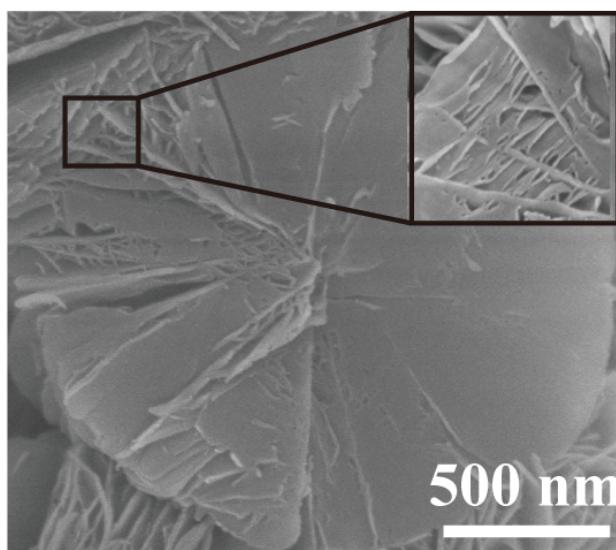


**Fig. S1.** SEM characterization of inner of the sample.

Experiments showed that the nucleation and growth rates of the flower-like structures formation were influenced by reaction temperature evidently. When decreased the reaction temperature to 30 °C, the solution kept clear until continuous stirring for more than 12 h and the nanopetals began to grow after stirring for about 24

h (Fig. S2a), which inferred that the nucleation and growth process of the sample proceeded very slowly at this temperature. Also, the yield of the product at this temperature was relatively low. Increase the reaction temperature to 50 °C, the rate of the process mentioned above improved significantly. The initial nanoflakes formed in 1 hour (Fig. S2c), and the flower-like structure can be formed in 3 hours. Elevating temperature to 80 °C, the formation of the nanoflakes and flower-like structures could be finished in 20 minutes (Fig. S2 d and e).

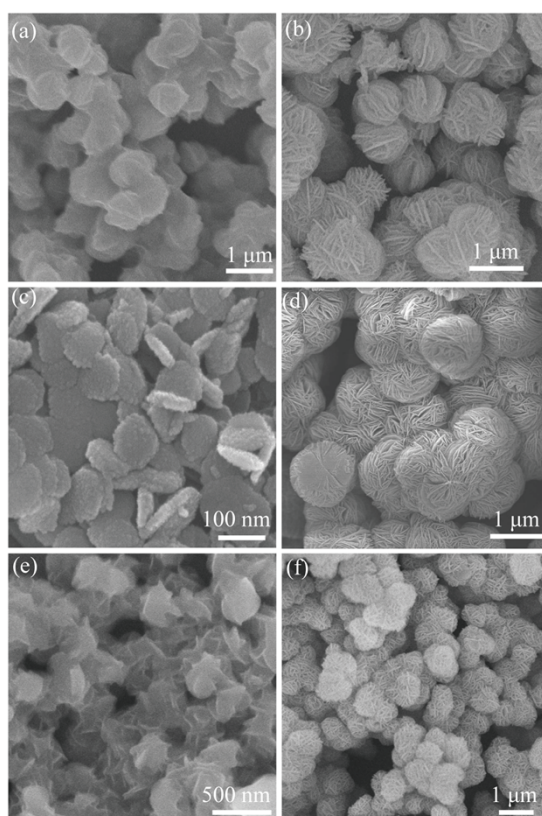


**Fig. S2.** SEM image of the product prepared at (a) 30 °C for 24 h; (b) 30 °C for 48 h; (c) 50 °C for 1 h; (d) 50 °C for 12 h; (e) 80 °C for 4 min; (f) 80 °C for 20 min.

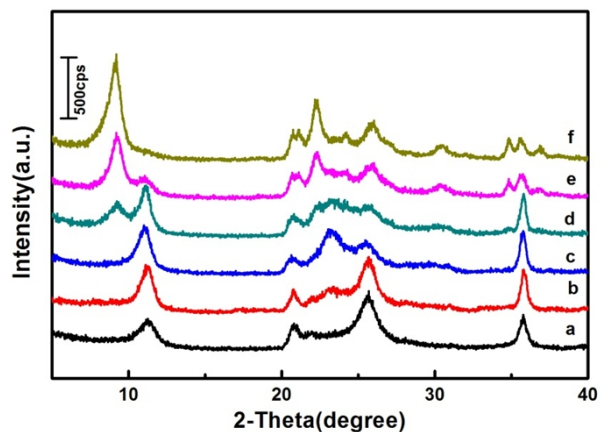


**Fig. S3.** XRD patterns of the products prepared at 50 °C of different reaction time

(a)12 h; (b) 24 h; (c) 36 h; (d) 48 h; (e) 60 h; (f) 84 h.

Reaction time was an important factor that affected the XRD patterns of the final product. As shown in Fig. S3, the diffractograms of the sample obtained at 12 h were in good agreement with  $\text{Ti}(\text{HPO}_4)_2 \cdot \text{H}_2\text{O}$ . When Increasing stir time to 48 h, a new peak at  $2\theta = 9.4^\circ$  appeared and increased continuously with extended reaction time. At the same time, the intense of the peak at  $2\theta = 11.6^\circ$  decreased and totally disappeared after stirring for 84h, the XRD patterns of the sample at this time was assigned to be  $\text{TiH}_2(\text{PO}_4)_2 \cdot 2\text{H}_2\text{O}$ .

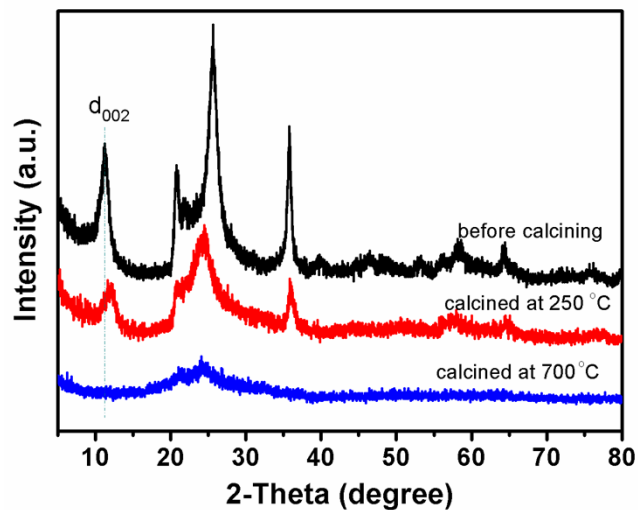


**Fig. S4.** XRD patterns of the products  $\text{Ti}(\text{HPO}_4)_2 \cdot \text{H}_2\text{O}$  before and after calcining at 250 and 700 °C.

As shown in Fig. S4, the collapse of the layered structure caused by the loss of the interlayer water can be seen from the shift of  $d_{002}$  peak and the  $\text{Ti}(\text{HPO}_4)_2 \cdot \text{H}_2\text{O}$  transform to  $\text{Ti}(\text{HPO}_4)_2$  after calcining at 250 °C. Increasing the calcined temperature to 700 °C, the crystal structure was totally destroyed due to the loss of both of interlayer and lattice water and transform to amorphous  $\text{TiP}_2\text{O}_7$ .

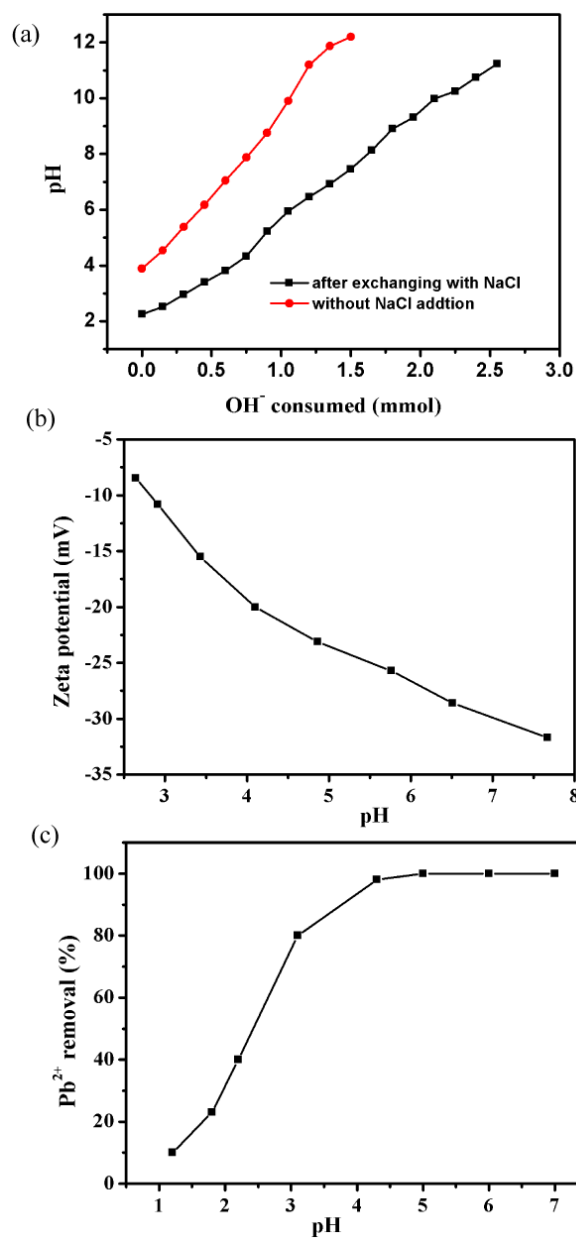


**Fig. S5.** (a) pH titration curves of titanium phosphate solution with and without  $\text{Na}^+$  exchanging. (b) plot of the zeta potential of the adsorbents as a function of pH. (c)  $\text{Pb}^{2+}$  removed efficiency of titanium phosphate as a function of pH. Experiments were conducted with initial lead concentration of  $10 \text{ mg}\cdot\text{L}^{-1}$  and sample dosage of  $5\text{mg}/25 \text{ mL}$ .



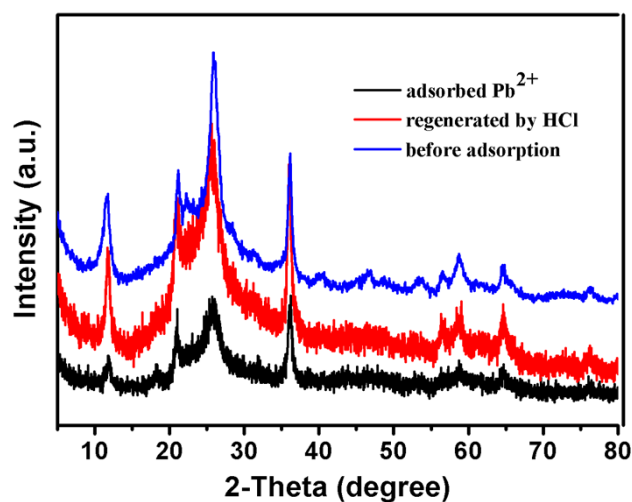


**Fig. S6.** XRD patterns of titanium phosphate before, after adsorption of Pb<sup>2+</sup> and regenerated by HCl.

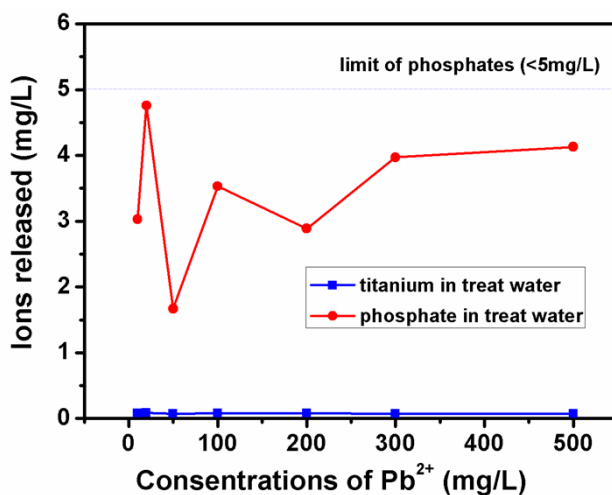


**Fig. S7.** Titanium and phosphates concentrations in treated water with different Pb<sup>2+</sup> concentrations, the initial Pb<sup>2+</sup> ion concentrations are 10~500 mg·L<sup>-1</sup> and adsorbent dose is 5 mg/25 mL.

We have analyze Pb in the solution after being treated with the adsorbents by ICP-MS ( NexION 300X, Perkinelmer) and the results are shown in table S1. It can be seen that if the lead ion concentration in water is lower than 5 ppm, which is still very high for lead ion polluted drinking water, the residual concentration of Pb<sup>2+</sup> ions is about 1.55 ppb, which is much lower than the drinking water standard for Pb (10 ppb).

**Table S1.** Pb<sup>2+</sup> remove performance at low lead concentrations.

Initial concentrations of Pb ( ppm )	10	5	3
Residual concentrations of Pb ( ppb )	11.7	1.55	1.15

(The adsorbent doses are 5 mg/25 mL, the initial concentrations of Pb<sup>2+</sup> are 10, 5, 3 mg L<sup>-1</sup>)

### Reference

- 1 X.-Y. Yu, R.-X. Xu, C. Gao, T. Luo, Y. Jia, J.-H. Liu and X.-J. Huang, *ACS Appl. Mat. Interfaces*, **2012**, 4, 1954; V. Rocher, J.-M. Siaugue, V. Cabuil and A. Bee, *Water Res.*, **2008**, 42, 1290.
2. K. Jia, B. Pan, Q. Zhang, W. Zhang, P. Jiang, C. Hong, B. Pan and Q. Zhang, *J. Colloid. Interf. Sci.*, 2008, 318, 160–166.
3. Q. R. Zhang, W. Du, B. C. Pan, B. J. Pan, W. M. Zhang, Q. J. Zhang, Z. W. Xu and Q. X. Zhang, *J. Hazard. Mater.*, 2008, 152, 469-475.